NOTES AND CORRESPONDENCE

Characteristics of the Recent Eastward Shift of Interannual NAO Variability

THOMAS JUNG, MICHAEL HILMER, EBERHARD RUPRECHT, AND SABINE KLEPPEK

Institut für Meereskunde, Universität Kiel, Kiel, Germany

SERGEY K. GULEV AND OLGA ZOLINA

P.P. Shirshov Institute of Oceanology, RAS, Moscow, Russia

21 June 2002 and 16 December 2002

ABSTRACT

Recent observational studies have shown that the centers of action of interannual variability of the North Atlantic Oscillation (NAO) were located farther eastward during winters of the period 1978–97 compared to previous decades of the twentieth century. In this study, which focuses on the winter season (December–March), new diagnostics characterizing this shift are presented. Further, the importance of this shift for NAO-related interannual climate variability in the North Atlantic region is discussed. It is shown that an NAO-related eastward shift in variability can be found for a wide range of different parameters like the number of deep cyclones, near-surface air temperature, and turbulent surface heat flux throughout the North Atlantic region. By using a near-surface air temperature dataset that is homogenous with respect to the kind of observations used, it is shown that the eastward shift is not an artifact of changes in observational practices that took place around the late 1970s. Finally, an EOF-based Monte Carlo test is developed to quantify the probability of changes in the spatial structure of interannual NAO variability for a relatively short (20 yr) time series given multivariate ''white noise.'' It is estimated that the likelihood for differences in the spatial structure of the NAO between two independent 20-yr periods, which are similar (as measured by the angle and pattern correlation between two NAO patterns) to the observed differences, to occur just by chance is about 18%. From the above results it is argued that care has to be taken when conclusions about long-term properties of NAO-related climate variability are being drawn from relatively short recent observational data (e.g., 1978–97).

1. Introduction

The North Atlantic Oscillation (NAO) is an atmospheric phenomenon that has been well-known to climate scientists for many decades. It has indirectly been discovered by its characteristic to induce simultaneous surface air temperature anomalies of different signs in west Greenland and northern Europe (e.g., Hann 1890). Depending on the sign of the anomalies this temperature seesaw is nowaday known as ''Greenland above'' and ''Greenland below'' mode, respectively (van Loon and Rogers 1978). While studying correlations between sea level pressure (SLP) time series from different stations worldwide Sir Gilbert Walker (Walker 1924) noticed that the Azores high and Icelandic low tend to strengthen and weaken simultaneously (see also Defant 1924). For this SLP seesaw, whose variations are accompanied by associated changes in the strength of the North Atlantic midlatitude westerly winds and subtropical trade winds, Walker introduced the term North Atlantic Oscillation.

In recent years the scientific interest in the NAO has increased considerably, fueled by a series of influential papers published in the early 1990s (e.g., Cayan 1992a; Deser and Blackmon 1993; Kushnir 1994; Hurrell 1995a). This increasing interest can be explained, among others, by NAO's strong impact upon regional climates in the North Atlantic region (Cayan 1992a; Hurrell 1995a), its influence on the North Atlantic Ocean (e.g., Bjerknes 1964; Curry et al. 1998; Eden and Jung 2001), and by its association with the observed Northern Hemisphere warming during the last decade (Hurrell 1996). More detailed overviews of the characteristics of the NAO are given, for example, in the review articles by Hurrell and van Loon (1997), Greatbatch (2000), and Wanner et al. (2001).

Much of what is known about the properties of the NAO and its impact on regional climates, however, is based on the assumption that the spatial structure of the NAO does not undergo temporal changes. While trying to understand why the link between the NAO and Arctic

Corresponding author address: Dr. Thomas Jung, ECMWF, Shinfield Park, Reading RG2 9AX, United Kingdom.
E-mail: thomas.jung@ecmwf.int

sea ice export through Fram Strait underwent changes around the late 1970s, Hilmer and Jung (2000) found out that the NAO centers of interannual variability were located farther eastward during the winters of 1978–97 (hereafter P2) compared to the winters of 1958–77 (hereafter P1). This finding has been confirmed by Lu and Greatbatch (2002). Jung and Hilmer (2001) went on to show that the spatial structure of interannual NAO variability during P2 was rather unusual in the context of the twentieth century. This recent change has been interpreted by Lu and Greatbatch (2002) in terms of an establishment of a new climate regime that accompanies an upward trend throughout the whole twentieth century in the correlation between the NAO and the dominant mode of the North Atlantic storm activity.

Eastward shifts of the NAO centers of action, which closely resemble the observed eastward shift, have also been found in experiments with general circulation models (GCMs) of different complexity. Peterson et al. (2002), for example, found an eastward shift of the centers of interannual NAO variability in hindcast integrations of a dry atmospheric GCM that has been forced with diagnosed diabatic forcing from the National Centers for Environmental Prediction–National Center for Atmospheric Research (NCEP–NCAR) reanalysis. Ulbrich and Christoph (1999) found an eastward shift of the NAO centers of action under increasing greenhouse gas concentrations in an integration of the coupled ECHAM/OPYC3 model, which closely resembles the observed shift (Jung 2000).

This study is an extension of previous papers by Hilmer and Jung (2000) and Jung and Hilmer (2001) and addresses four issues. First, the basic characteristics of the recent eastward shift of the NAO centers of action are briefly reviewed using new diagnostics. Second, it is shown how the response of regional climates to a forcing by the NAO has changed during the last 40 yr. This is done for the number of deep cyclones, near-surface air temperatures (SAT), and North Atlantic air–sea interaction (turbulent surface heat fluxes). Third, the statistical significance of the shift is assessed taking into account sampling issues that may be crucial when differences in the statistical characteristics of the NAO between two relatively short (20-yr) periods are considered. Finally, the results are discussed in a broader context and an attempt is made to pinpoint possible causes for the observed eastward shift.

2. Data

The main dataset used in this study comes from the NCEP–NCAR reanalysis (Kalnay et al. 1996). This project aims to reduce analysis inhomogeneties that arise from changes in the model that are used in data assimilation to produce analysis fields on an operational basis. It is worth noting in the context of the present study that Kistler et al. (2001) found the quality of the analysis (measured in terms of the difference between 6-h forecasts and the analysis) of the Northern Hemisphere atmospheric flow to be uniform throughout the reanalysis period. Here we use 6-h SLP fields from the reanalysis to determine North Atlantic cyclone characteristics. The focus is on deep cyclones (deeper than 980 hPa) to reduce tracking uncertainties that are particularly prominent for relatively weak low pressure systems. Cyclone counts were derived using the semiautomatic tracking procedure by (Grigoriev et al. 2000). All results were normalized with respect to the box size at 45°N ($\approx$218 000 km^2). Further details about this dataset and its application in the context of climate variability are given elsewhere (Gulev et al. 2001).

The NAO index used in this study is the difference between normalized observed SLP time series from Lisboa and Iceland (Hurrell 1995a). We have also used a NAO index based on NCEP–NCAR reanalysis data for all diagnostics performed for the period 1958–97. The latter index is based on SLP data from those grid points closest to the Azores and Iceland. For this period no dependence of the conclusions on the particular choice of the index has been found. All subsequent results are based on the former NAO index.

Additionally, an updated version of monthly mean SLP analyses from (Trenberth and Paolino 1980) has been used. Up to 1962 these data are based on historical weather charts. Thereafter operational analyses from U.S. Navy and NCEP analyses were used. Note, that this dataset, albeit (slightly) different from the reanalysis, still includes time-dependent changes in the observational practice, like, for example, increasing use of satellite data from 1979 to present.

To study the influence of the NAO's eastward shift on SAT we used two datasets. The first SAT dataset is based 2-m air temperature data taken from the NCEP–NCAR reanalysis. Since this parameter is partly influenced by model physics (Kistler et al. 2001), and since SAT from the reanalysis is influenced by changes in the observational procedures, we also used direct observations from a variety of stations worldwide (Jones and Moberg 2003). Since the latter dataset is solely based on direct observations, it is used to indirectly (via the response of SAT to the NAO) test whether the eastward shift is an artifact due to changes in the observing practices that were most pronounced around the late 1970s (Kistler et al. 2001).

Moreover, turbulent surface heat fluxes from the NCEP–NCAR reanalysis are used. The surface fluxes are completely determined by the model subject to the constraint of the assimilation of other observations (Kistler et al. 2001). A comparison of reanalyzed fluxes with estimates from voluntary observing ship (VOS) data reveals that the dominant modes of variability are very similar for both datasets in well-sampled regions. Differences are evident, however, in remote regions like the Labrador Sea region, which may partly be explained by differences in ''sampling'' (S. K. Gulev 2002, personal communication), that is, the NCEP–NCAR re-

analysis also gives dynamically consistent values in poorly sampled region through constraints by the (relatively well known) large-scale atmospheric flow.

Finally, SLP data from a 300-yr control integration of the coupled atmosphere–ocean–sea ice model ECHAM4/OPYC3 under present-day climate conditions is being used (Roeckner et al. 1996). The atmospheric component ECHAM4 is the fourth generation of a hierarchy of model that has been developed at the Max Planck Institute for Meteorology, Hamburg, Germany, from the former European Centre for Medium-Range Weather Forecasts (ECMWF) model (Roeckner et al. 1992, 1996). ECHAM4 is a spectral model at T42 ($\approx 2.8° \times 2.8°$) with 19 hybrid levels in the vertical. OPYC3 is a three-component model including an (isopycnial) interior ocean, a mixed layer component, and a dynamic–thermodynamic sea ice model. ECHAM4/OPYC3 has been diagnosed in a wide range of NAO-related studies (e.g., Ulbrich and Christoph 1999; Christoph et al. 2000; Jung and Hilmer 2001).

3. Results

a. Changes of interannual NAO variability

To describe the eastward shift of the NAO centers of interannual NAO variability we follow Hilmer and Jung (2000), that is, detrended SLP anomalies were regressed onto the detrended and normalized NAO index (Fig. 1). In contrast to the study by Hilmer and Jung (2000), though, our results are based on the updated SLP dataset from Trenberth and Paolino (1980). The similarity to the results by Hilmer and Jung (2000; their Fig. 4) shows that the recent shift of interannual NAO variability is not an artifact of the NCEP–NCAR reanalysis. This comparison does not clarify, however, whether the shift results from the use of satellite data after 1978, which may influence both datasets. Pronounced differences between P2 and P1 are evident for NAO-related geostrophic wind anomalies, particularly in the Greenland Sea, the Labrador Sea region, and over large parts of the European continent (Fig. 1c). While the magnitude of these differences is smaller in the subtropics so is the magnitude of interannual atmospheric variability in low latitudes.

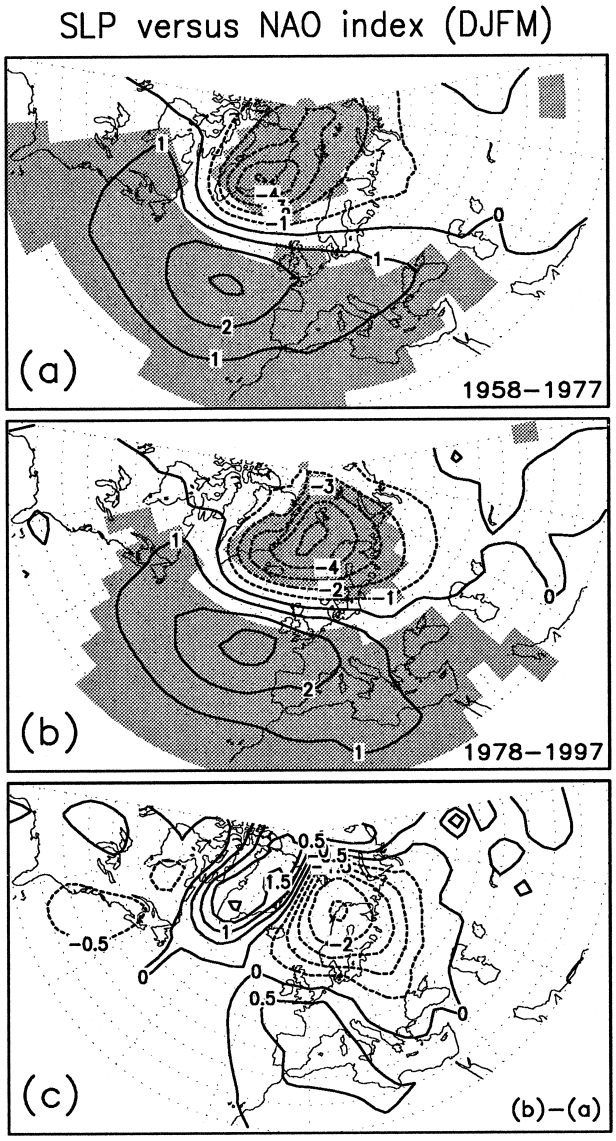

FIG. 1. SLP anomalies (hPa) that are associated with the NAO index during winters [December–March (DJFM)]: (a) 1958–77 and (b) 1978–97. SLP anomalies were regressed onto the normalized NAO index. Linear trends were removed beforehand. Statistically significant slope parameters (at 95% confidence) are shaded. (c) Difference between (b) and (a).

So far the conclusions are based on the use of the NAO index, which is defined at fixed locations. One might argue that changes in the spatial structure of a natural mode of atmospheric variability may not effectively be described by such an index. To circumvent the subjectivity that comes with the choice of an index, we performed empirical orthogonal function (EOF) analysis of detrended, winter-averaged North Atlantic SLP anomalies from the NCEP–NCAR reanalysis data for the two periods P1 and P2. [Very similar EOFs are obtained for SLP data from Trenberth and Paolino (1980).] The first EOFs for each of the periods P1 and P2 (Fig. 2) are well separated from subsequent modes according to the criterion of North et al. (1982) and closely resemble the associated regression patterns shown in Fig. 1. This similiarity is particularly evident for the difference between the leading EOFs (cf. Figs. 1c and 2c). Thus, we are confident that the NAO index can be used to describe the eastward shift in an efficient manner.

The above results are based on the usage of linearly detrended data. In order to check whether the changes in the spatial structure of interannual NAO variability are influenced by detrending the data, we have computed EOFs for the original data as well (no trend has been removed). The leading EOFs are virtually the same as

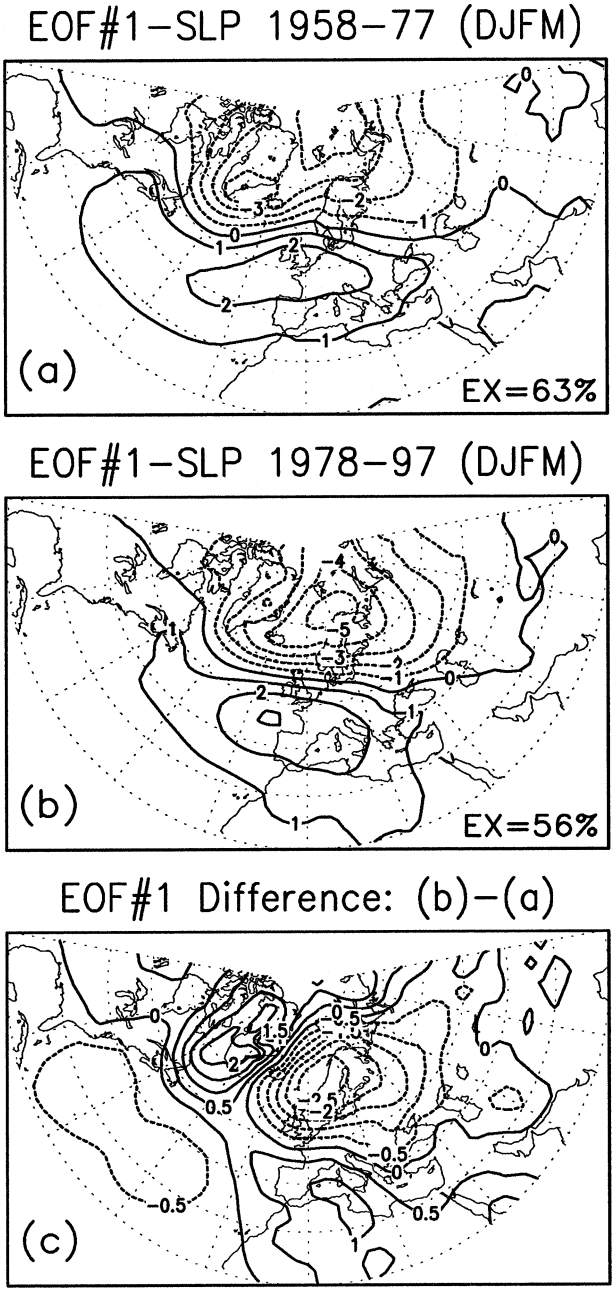

FIG. 2. First EOF of detrended wintertime (DJFM) North Atlantic SLP anomalies (hPa) for the period (a) 1958–77 and (b) 1978–97. (c) Difference between (b) and (a). The first EOF explains 63% and 56% of the variance in (a) and (b), respectively.

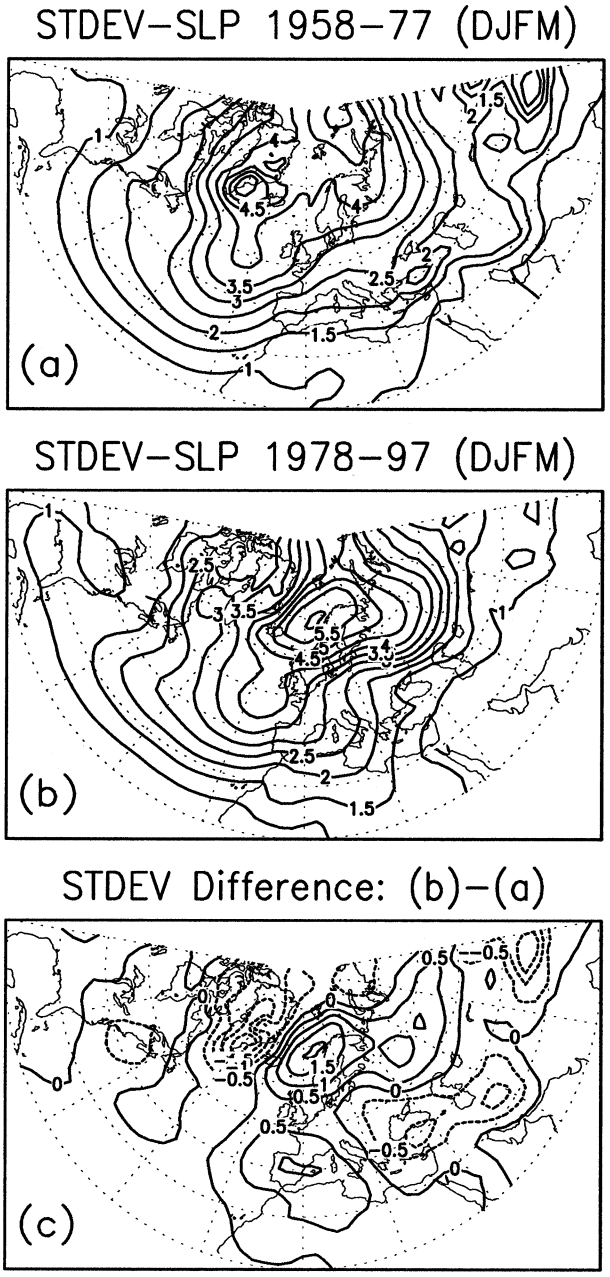

FIG. 3. Std dev of North Atlantic SLP anomalies (hPa) for the period (a) 1958–77 and (b) 1978–97. (c) Difference between (b) and (a).

those obtained using detrended data (not shown). Obviously, the detrending procedure does not influence the basic characteristics of the observed eastward shift.

From the above results it is not clear whether the NAO-related changes in the spatial structure from P1 to P2 were the only changes taking place in the North Atlantic region. From Fig. 3, which shows the standard deviation of North Atlantic SLP for P1 and P2 along with the difference of the standard deviations between P2 and P1, it becomes clear that the main differences in the total standard deviation is due to the eastward shift of the centers of interannual NAO variability. From this diagnostic there is no indication of changes of the spatial structure of other teleconnection patterns, at least in the North Atlantic region.[1]

[1] It is worth mentioning, though, that the centers of interannual variability of the Aleutean low pressure system also underwent an eastward shift around the late 1970s (Jung 2000).

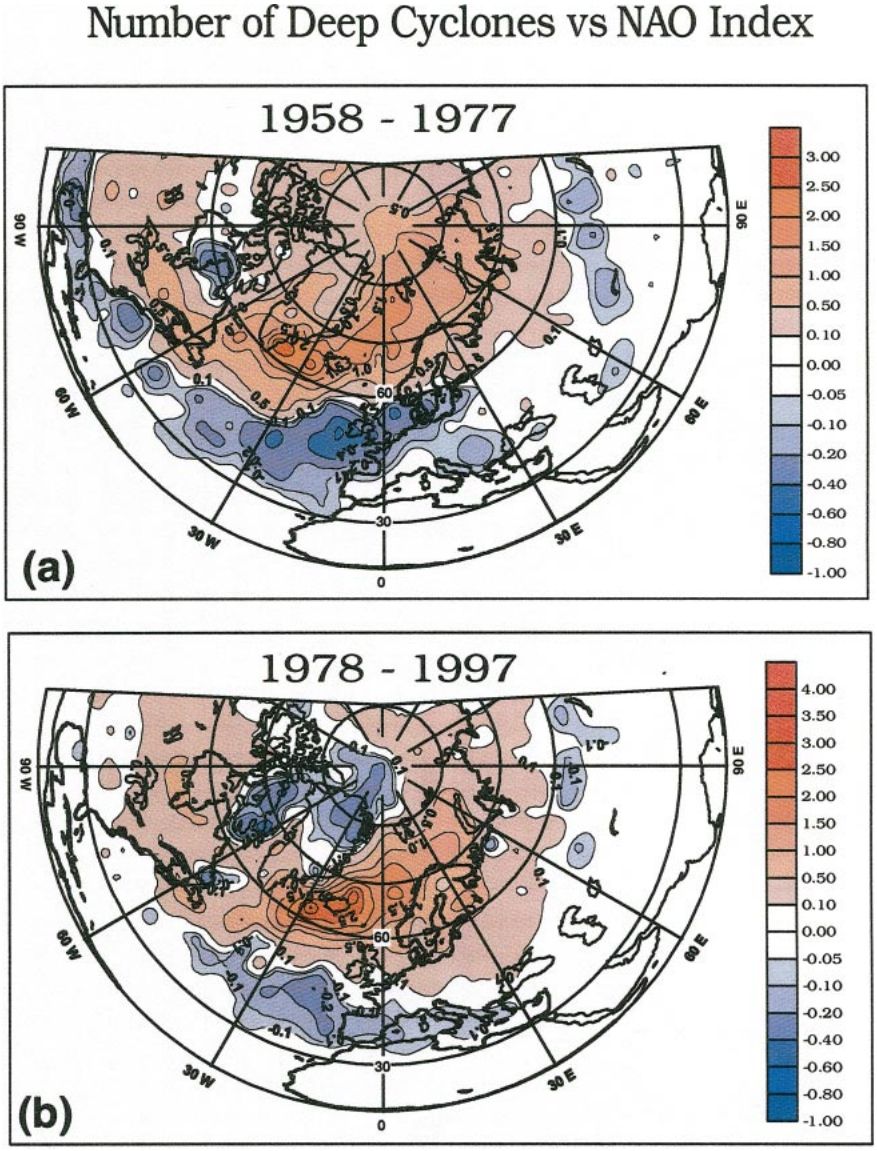

FIG. 4. As in Fig. 1, except for anomalies of the number of deep (<980 hPa) cyclones per winter (in number of cyclones per season).

b. Associated changes

1) NUMBER OF DEEP CYCLONES

It is well known that high and low NAO winters are accompanied by changes in the cyclone activity over the North Atlantic region (e.g., Hurrell 1995b; Gulev et al. 2001, 2002). Thus we can expect that the eastward shift of the NAO centers of interannual variability is also evident for NAO-related North Atlantic cyclone activity (Gulev et al. 2001, 2002). Spatial patterns of the anomalous number of deep cyclones (deeper than 980 hPa) that are associated with interannual NAO variability for each of the periods P1 and P2 are shown in Fig. 4. During the earlier period P1 the main NAO-related deep cyclone track was aligned from the Labrador Sea, over Iceland into the Arctic. Intensification of this track was accompanied by a decreasing number of deep cyclones from the eastern seaboard toward northwestern Europe, particularly west of the United Kingdom. During the later period P2 the main NAO-related high-latitude storm track was more confined to the Icelandic region and more zonally oriented. As a result of this shift, for instance, the probability of occurrence of NAO-related deep cyclones over middle Europe was reduced (enhanced) for high NAO winters during P1 (P2). Moreover, the NAO influenced the occurrence of deep Mediterranean cyclones only during the last two decades. During P1, on the other hand, the NAO exerted little control on the number of deep cyclones in the Mediterranean region.

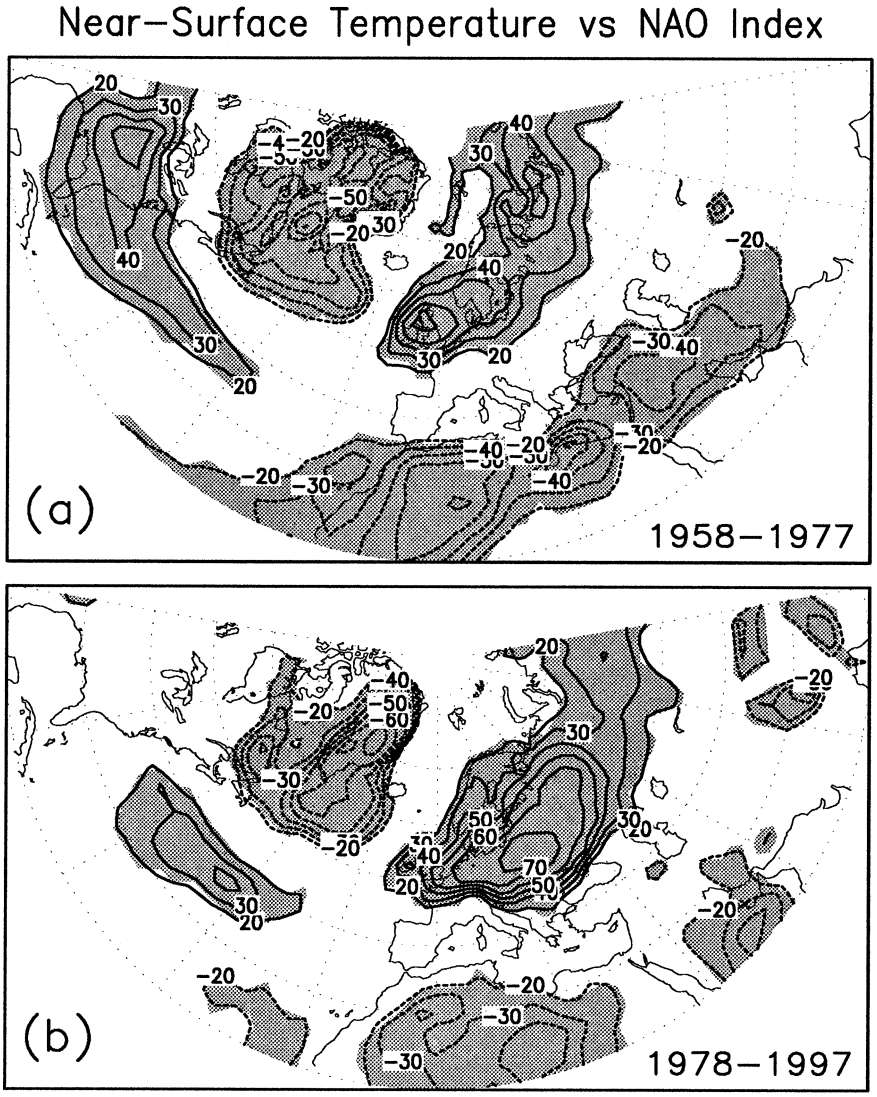

FIG. 5. Local correlations [$r^2 \times 100 \times \text{sgn}(r)$ in %] between winter-averaged (DJFM) SAT anomalies and the NAO index for the period (a) 1958–77 and (b) 1978–97. Linear trends were removed beforehand. The sign of the correlation enters via sgn(r). The contour interval is 10% for magnitudes exceeding 20% (shaded).

2) SURFACE AIR TEMPERATURE

It has long been noticed that high and low NAO winters are accompanied by SAT anomalies over the neighboring continents (Loewe 1966; van Loon and Rogers 1978; Hurrell and van Loon 1997). In the long-term context (1864–1994) high NAO winters, for example, are accompanied by anomalously high SAT over northern Europe, eastern Russia, and the southeastern United States; at the same time the northwestern part of the North Atlantic region and regions south of the Mediterranean face anomalously cold conditions (Hurrell and van Loon 1997, their Fig. 6). This long-term SAT response to a forcing by the NAO resembles the response pattern for P1 (Fig. 5a). During P2 the NAO exerted no significant influence on SAT anomalies over the southeastern United States, whereas the percentage of SAT variance explained by the NAO over eastern Europe (e.g., Poland and Ukraine) increased considerably compared to P1 (Fig. 5b). The fact that the response of SAT anomalies to the NAO during P1 has a closer resemblence to the long-term SAT response (1864–1994) compared to P2 indirectly supports the conclusion by Jung and Hilmer (2001), that is, the spatial structure of interannual NAO variability as observed during the last two decades is rather unusual. Differences in the SAT response between P2 and P1 can be explained by an increase (decrease) of the NAO-related zonal (meridional) flow over Europe (southeastern United States) from P1 toward P2 (Fig. 1). Similar arguments are evident for changes of the SAT response over eastern Canada and parts of Greenland.

TABLE 1. Linear cross-correlation coefficients between the NAO index and near-surface air temperature measurements at different stations. Results for wintertime data (DJFM) and three different periods (1958–77, 1978–97, and 1866–1957) are given. For the former two periods the correlations for raw/detrended data are also given. For the period 1866–1957 the correlation coefficients are given only for those stations for which all data were available.

Station	Location	Correlation		
		1958–77	1978–96	1866–1957
Oslo (Norway)	60.0°N, 10.7°E	+0.67/+0.76	+0.68/+0.72	+0.54
Stockholm (Sweden)	59.3°N, 18.1°E	+0.70/+0.77	+0.73/+0.76	+0.68
Edinburgh (United Kingdom)	56.0°N, 3.4°W	+0.61/+0.67	+0.79/+0.85	—
Copenhagen (Denmark)	55.7°N, 12.6°E	+0.74/+0.78	+0.80/+0.82	+0.62
De Bilt (Netherlands)	52.1°N, 5.2°E	+0.62/+0.71	+0.83/+0.86	+0.53
Brussels (Belgium)	50.8°N, 4.4°E	+0.65/+0.73	+0.80/+0.82	+0.49
Hamburg (Germany)	53.6°N, 10.0°E	+0.70/+0.78	+0.84/+0.86	—
Zurich (Switzerland)	47.4°N, 8.6°E	+0.44/+0.47	+0.70/+0.74	+0.25
Vienna (Austria)	48.2°N, 16.4°E	+0.64/+0.73	+0.79/+0.80	+0.42
Warsaw (Poland)	52.2°N, 21.0°E	+0.65/+0.72	+0.87/+0.88	+0.49
St. Petersburg (Russia)	60.8°N, 30.3°E	+0.62/+0.69	+0.77/+0.79	+0.54
Charleston, WV	38.4°N, 81.6°W	+0.70/+0.79	+0.39/+0.51	+0.37
Springfield, IL	39.8°N, 89.7°W	+0.78/+0.84	+0.41/+0.52	—
Resolute (Canada)	74.7°N, 95.0°W	−0.63/−0.65	−0.26/−0.37	—
Godthaab (Greenland)	64.2°N, 51.8°W	−0.81/−0.86	−0.68/−0.73	—

As mentioned in section 2 SAT data from the NCEP–NCAR reanalysis are influenced by model physics and changes in observational practices, in particular through the increasing usage of satellite data from the late 1970s onward. To test whether our conclusions are influenced by these issues, correlation coefficients between the NAO index and direct SAT time series from meteorological stations were computed for three different periods, that is, 1958–77, 1978–97, and 1866–1957 (Table 1). For the former two periods correlation coefficients were computed, both for detrended and raw data. It becomes obvious from Table 1 that similar changes in the link between the NAO and SAT anomalies can be found for NCEP–NCAR reanalysis data (Fig. 5) and the direct observations. Moreover, our conclusions are not affected by detrending the data. Consistent with the results for the NCEP–NCAR reanalysis data, considerable changes in the link from P1 and P2 can be found, for example, in wide parts of Europe (De Bilt, Netherlands; Zurich, Switzerland; and Warsaw, Poland) and in the United States (Charleston, South Carolina; and Springfield, Illinois). Finally, correlation coefficients for the period 1866–1957 over Europe are closer to those obtained for P1 than for P2. The same holds for Charleston, West Virginia. This comparison, thus, supports the conclusion by Jung and Hilmer (2001) that the structure of interannual NAO variability during P2 was rather unusal in a long-term context (1866–1977).

3) TURBULENT SURFACE HEAT FLUXES

Recent modeling studies suggest that the North Atlantic Ocean circulation is particularly sensitive to NAO-related turbulent surface heat flux anomalies in the Labrador Sea region (e.g., Eden and Jung 2001; Eden and Willebrand 2001); NAO-related turbulent surface heat flux anomalies in the Labrador Sea lead to changes in the (oceanic) convective activity and, after some delay, to changes of the North Atlantic circulation (Eden and Willebrand 2001). Given the importance of NAO-related turbulent heat flux variations for the North Atlantic Ocean circulation, they have been separately estimated for the two periods P1 and P2. Differences in the turbulent surface heat flux response to a forcing by the NAO on interannual timescales between P1 to P2 are strongest over the western part of the North Atlantic basin (Fig. 6), a region where climatological temperature and humidity contrasts are most pronounced. On average, high NAO winters (one standard deviation above the average), for instance, were accompanied by turbulent surface heat flux anomalies out of the northwestern North Atlantic Ocean (see also Cayan 1992a). For high NAO winters (one standard deviation above the average) these anomalies exceeded 70 W m^{-2} during P1 in the central Labrador Sea. During P2, however, the same NAO anomalies were accompanied by heat flux anomalies that were reduced by about a factor of 2 compared to P1. These differences are in line with our physical understanding of air–sea interaction. High (low) NAO winters are accompanied by enhanced (reduced) geostrophic northwesterly winds, enhanced (reduced) cold air advection, and enhanced (reduced) dry air advection, all which give rise to enhanced (reduced) turbulent heat fluxes out of the ocean (e.g., Cayan 1992b). Since the influence of interannual NAO variability on turbulent heat flux anomalies in the Labrador Sea region has diminished from P1 to P2 (Fig. 6), one might expect, therefore, that the response of the North Atlantic circulation to a turbulent heat flux forcing by the NAO has also weakened from P1 to P2. Similar arguments may explain changes of NAO-related turbulent surface heat flux anomalies in the western subtropical basin and in the Icelandic Sea.

It is worth mentioning that the average extension of

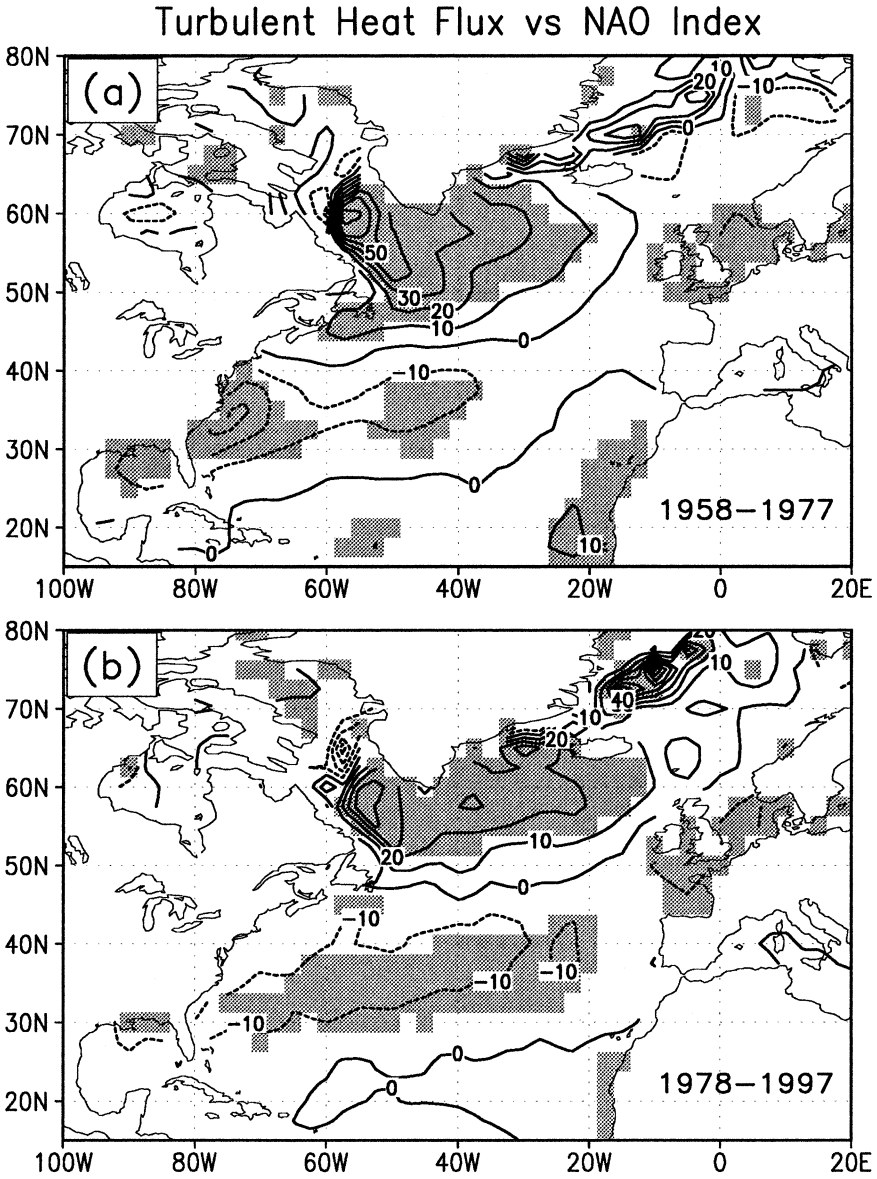

FIG. 6. As in Fig. 4, except for turbulent surface heat flux anomalies (W m^{-2}). Positive values are directed out of the ocean. Statistically significant slope parameters (at 95% confidence) are shaded.

the sea ice cover was larger (smaller) in the Labrador Sea region (Nordic Seas region) during P2 compared to P1 (Deser et al. 2000). Aside from an influence on the mean fluxes this secular change has an influence on the turbulent heat flux response to a forcing by the NAO, particularly close to the ice edge. This is due to the fact that turbulent surface heat flux variability is lower over ice-covered areas than over the ocean. Given the arguments described above, though, we expect differences in turbulent heat fluxes in Fig. 6 relative to the sea ice edge to be a result of changes in the NAO-related atmospheric flow. Note also in this context the changes off the southeastern U.S. seaboard from P1 to P2.

c. Inference

So far no attempt has been made in order to quantify how unusual the observed eastward shift of the NAO centers of action is, given a simple null hypothesis (sampling variability). In this section a Monte Carlo procedure is used in order to quantify how unusual the difference between the first EOFs (NAO) for the two periods P1 and P2 (Fig. 2) is. This test takes into account that EOF analysis, like other statistical techniques, is subject to sampling fluctuations (e.g., Cheng et al. 1995).

Suppose we have a long multivariate time series $\mathbf{x}(t)$,

with time $t = 1, \ldots, T$. In the context of the present study $\mathbf{x}(t)$ represents North Atlantic SLP anomalies. By diagnonalizing the corresponding covariance matrix $\mathbf{C}_x$, we obtain the EOFs (eigenvectors) $\mathbf{e}^i$, where i denotes the ith eigenmode. The first EOF ($i = 1$), which represents the NAO, explains most of the variance of the original dataset. Higher-order modes explain increasingly less variance and are subject to an orthogonality constraint. The variance that can be explained by the ith eigenmode is given by the normalized eigenvalues $\lambda^{\dagger i} = \lambda^i / \Sigma_i \lambda^i$. The principal components $\alpha^i(t)$ represent the new coordinates in EOF space and are obtained by projecting the anomalies $\mathbf{x}(t)$ back onto the EOFs. Here, without any loss of generality, we choose the principal components (PCs) to be orthonormal, that is, $\Sigma_t \alpha^i(t)\alpha^j(t) = \delta_{ij}$, where δ_{ij} is Kronecker's delta. Note, that the normality of the PCs means that the EOFs carry the units. The anomalies can be reconstructed as follows:

$$\mathbf{x}(t) = \sum_{i=1}^{M} \alpha^i(t)\mathbf{e}^i, \tag{1}$$

where $M = \min(T, L)$ denotes the number of eigenmodes and L is given by the number of grid points. We split up the time series of the PCs into K subsamples. Then Eq. (1) can be written as follows:

$$\mathbf{x}(t) = \sum_{i=1}^{M} \alpha^i(t_1)\mathbf{e}^i + \sum_{i=1}^{M} \alpha^i(t_2)\mathbf{e}^i + \cdots + \sum_{i=1}^{M} \alpha^i(t_K)\mathbf{e}^i, \tag{2}$$

$$= \mathbf{x}(t_1) + \mathbf{x}(t_2) + \cdots + \mathbf{x}(t_K), \tag{3}$$

$$= \sum_{k=1}^{K} \mathbf{x}(t_k), \tag{4}$$

where $t_1 = 1, \ldots, N$, $t_2 = N + 1, \ldots, 2 \times N$, and $t_K = N \times K - N + 1, \ldots, K \times N$. Here, N gives the length of the K subsamples of $\mathbf{x}(t)$ ($N = 20$ yr, in this study). In this study difference between the first EOFs of two such subsets, say $\mathbf{e}_1^1$ and $\mathbf{e}_2^1$, are compared. For the original time series $\mathbf{x}(t)$ the PCs are uncorrelated by construction. When we consider subsets of this dataset, however, then correlations between different PCs may be found. Jung and Hilmer (2001), for example, estimated that the likelihood to find correlations higher than 0.47 for two 20-yr chunks of (uncorrelated) ''white noise'' is about 2.5%. These correlations arise just by chance due to the use of relatively short segments of white noise. If the EOFs for one subset, say $\mathbf{x}(t_1)$, are computed, then by chance correlations between different PCs due to sampling variability may result in EOFs $\mathbf{e}_1^i$ that are different from the original, ''true'' EOFs $\mathbf{e}^i$. Therefore, sampling variability may be seen as the simplest explanation for the observed differences between the first EOFs of North Atlantic SLP anomalies for P1 and P2 shown in Fig. 2.

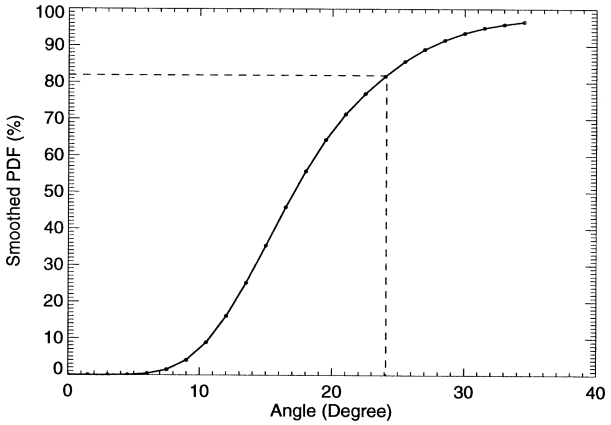

FIG. 7. Cumulative smoothed PDF of the angles between the first EOFs for two randomly chosen independent 20-yr periods of multivariate white noise. The angles were determined using an Euclidean norm. A Gaussian kernel with a window width of 1.5° has been used for smoothing. The dashed lines mark values for the observed angle between the first EOFs for P1 and P2. To avoid problems due to the nonunique sign of the EOFs, the angles were computed for EOFs representing the positive phase of the NAO.

To quantify the likelihood to obtain observed differences between the first EOFs for P1 and P2 just by chance, the following Monte Carlo test is used. In order to describe spatial covariations of the observed North Atlantic SLP anomalies the EOFs for period 1948–2002 ($\hat{\mathbf{e}}_1^i$) are used. The choice of this relatively long period for the decomposition leads to a more representative eigenvalue spectrum, which is crucial for the outcome of the test. The first and second EOFs of North Atlantic SLP anomalies explain 54.6% and 13.8% of the total SLP variance for the period 1948–2002, respectively. Then, the PCs $\alpha_1^i(t)$ are replaced by pseudo-PCs $\tilde{\alpha}_1^i(t)$, which are obtained from independent realizations of white noise. The choice of white noise instead of serially correlated ''red noise'' is motivated by the fact that the leading PCs for P1 and P2 of observed, detrended SLP anomalies show no significant autocorrelations. Next, 1000 independent pairs of surrogate datasets have been contructed from the EOFs for P1 and the pseudo-PCs as follows:

$$\tilde{\mathbf{x}}_1^{\mu}(t_1) = \sum_{i=1}^{M} \tilde{\alpha}^{i\mu}(t_1)\hat{\mathbf{e}}_1^i \tag{5}$$

$$\tilde{\mathbf{x}}_2^{\mu}(t_2) = \sum_{i=1}^{M} \tilde{\alpha}^{i\mu}(t_2)\hat{\mathbf{e}}_1^i, \tag{6}$$

with $t_1 = t_2 = 1, \ldots, 20$ and $\mu = 1, \ldots, 1000$. For each of these surrogate datasets the first EOFs $\tilde{\mathbf{e}}_1^{1\mu}$ and $\tilde{\mathbf{e}}_2^{1\mu}$ were determined. The cumulative probability density function (PDF) of the angles between the first EOFs from the surrogate datasets are depicted in Fig. 7 along with the observed angle of 24.1°. The Euclidean norm

has been used to determine the angles. As can be seen from Fig. 7, the likelihood that the observed angle (and therefore the eastward shift) is due to sampling variability is about 18%. The same conclusion is obtained if the pattern correlation coefficient is used to measure the difference between the first EOFs (not shown).

One might argue that the above Monte Carlo test yields surrogate atmospheric flow patterns that are dynamically not very reasonable, due to the unconstraint superposition of different EOFs. Therefore, a related test has been performed for the coupled ECHAM4/OPYC3 model. The first, second, and third EOF for the whole 300-yr period explain 55.6%, 9.7%, and 8.5%, respectively, of the total SLP variance. Obviously, the eigenvalue spectrum for the coupled model is very similar to those for the NCEP–NCAR data for the period 1948–2002 (see above). Next, the EOFs of North Atlantic SLP anomalies were separately computed for all 15 nonoverlapping 20-yr periods from the 300-yr integration of the coupled model. Then, the angles and spatial correlation coefficients (r_s) for all different combinations of the first EOFs of the 20-yr subsamples were computed. It was found that the angle (r_s) is larger (smaller) than the observed angle (r_s) between the first EOFs for P1 and P2 for 27 (24) pairs out of a total of 105 pairs. This shows that differences between the first EOFs of independent 20-yr subsamples for the coupled model are very similar to those for the surrogate dataset.

It is worth stressing that both measures, the angle and the pattern correlation coefficient, are ''blind'' with respect to the details of the differences between the first EOFs. That is, the PDF of the angles shown in Fig. 7 account not only for eastward shifts, but for all different kind of spatial changes. This more general test is necessary to perform because Hilmer and Jung (2000) did not have any a priori expectation for the NAO to shift *eastward.*

4. Discussion

During the winters of the last four decades the NAO underwent two different kinds of interdecadal changes. First, the NAO showed the well-known pronounced positive trend from predominantly low values during the 1960s to predominantly high values during the 1990s (Hurrell 1995a). Second, this trend came along with an eastward shift of the NAO centers of interannual variability (Hilmer and Jung 2000). Based on direct SAT observations and the NAO index it is shown that the shift is not an artifact resulting from changes in observational practices that took place around the late 1970s (e.g., increasing use of satellite data). In fact, the observed eastward shift appears to be part of a series of secular changes that took place around the late 1970s, for example, the change from low to high values of the NAO (Hurrell 1995a) and the Pacific North American pattern (Trenberth and Hurrell 1994), the increase of Northern Hemisphere mean temperatures (e.g., Hurrell 1996), the eastward shift of the centers of action of interannual variability of the Azores low pressure system (Jung 2000), changes in the link between the polar night jet and the tropospheric NAO (Kodera et al. 1999), and changes in the characteristics of the El Niño–Southern Oscillation phenomenon (e.g., Wang 1995).

What are the causes for the observed eastward shift of the NAO centers of action during the last two decades? From the results of the Monte Carlo test presented in this study, a plausible explanation for the shift is sampling variability. Obviously, for relatively short time segments (20 yr), the NAO may mix with other modes of SLP variability (higher-order EOFs) giving rise to considerable spatial deviations from the long-term structure of the NAO. It is worth noting, however, that recent modeling studies suggest that there may be other causes for the observed eastward shift. Ulbrich and Christoph (1999), for example, found an eastward shift of the NAO, which closely resembles the observed eastward shift, under increasing greenhouse gas concentrations in the coupled ECHAM4/OPYC3 model, suggesting that increasing greenhouse gas concentrations are the cause for the observed shift. It seems worthwhile to test this hypothesis by diagnosing corresponding integrations of coupled GCMs from other centers in this context. There is another parallel between the results by Ulbrich and Christoph (1999) and the observations, that is, the eastward shift was accompanied by an increase in the strength of the mean westerly winds in the North Atlantic region. The study by Peterson et al. (2002) suggests that indeed secular changes in the strength of the mean westerly flow lead to changes in the spatial structure of interannual NAO variability. Peterson et al. (2002) forced a dry primitive equation model with a NAO-related diabatic proxy forcing for the period 1958–97. Their spatial forcing pattern is fixed over the whole period; the magnitude of the forcing is determined by the observed NAO index. Using this experimental setup Peterson et al. (2002) were able to reproduce the observed eastward shift. From these results they draw two conclusions. First, the shift is a nonlinear phenomenon; the response (changed spatial structure) does not simply mirror the forcing (fixed spatial structure). Second, the secular increase of the NAO during the last four decades is the driving mechanism, since the only difference between their forcing during 1958–77 and 1978–97 is a marked difference associated with the strength of the background flow. This interpretation seems to be consistent with the modeling study by Simmons et al. (1983), which shows that the centers of low-frequency intraseasonal teleconnection patterns are determined by the location of the diffluent part of the jet stream (see also Nakamura 1996, for observational evidence). Since the trend toward a positive NAO was accompanied by an eastward extension of the mean jet exit regions, this may have led to eastward shift of the centers of low-frequency intraseasonal NAO variability, which, through aliasing (Madden and Jones

2001), may have led to the observed eastward shift of the NAO centers of interannual variability.

It might come as a surprise in this context that the centers of interannual NAO variability were not displaced during the first two decades of the twentieth century albeit the fact that the NAO was prevalently in its positive phase (Jung and Hilmer 2001). At first glance this appears to be contradictory to the hypothesis that the strength of the background flow governs the spatial structure of interannual NAO variability. An explanation for this apparent contradiction has been provided by Peterson et al. (2003). By using the same experimental setup as Peterson et al. (2002), they were able to show that in their model the longitudinal position of the centers of interannual NAO variability depends nonlinearly on the strength of the background flow. While for moderate anomalies of the background flow (NAO) the centers of interannual NAO are stable, it is for *large* positive (negative) anomalies above one standard deviation (below minus two standard deviations) only that the centers shift toward the east (west). Thus, the fact that a shift of the centers of interannual NAO variability is evident for the last two decades might be explained by the unusually large change toward prevalently positive values of the NAO.

Whatever the mechanism for the observed eastward shift of interannual NAO variability is, its importance is stressed by its strong influence on NAO-related variability for a variety of parameters like, for example, the sea ice volume exports through Fram Strait, Denmark Strait, and Davis Strait (Hilmer and Jung 2000), the number of deep cyclones, near-surface air temperatures, and air–sea interaction. We expect, by inference, that other parameters (e.g., precipitation and North Atlantic wave height) were also affected by these changes. The unusual structure of interannual NAO during the last two decades suggests that care has to be taken when the NAO-related climate variability is studied using data from recent decades only. An instructive example in this context is the changing link between the NAO and the sea ice export through Fram Strait (Kwok and Rothrock 1999; Dickson et al. 2000; Hilmer and Jung 2000; Jung and Hilmer 2001). Similar problems may arise, for example, when paleoclimate proxies are calibrated or statistical downscaling models are estimated from relatively short (recent) datasets.

Acknowledgments. Helpful discussions with Richard Greatbatch, Drew Peterson, and Jian Lu are very much appreciated. Comments by two anonymous reviewers were very helpful in clarifying the conclusions of the manuscript. Phil Jones kindly provided the near-surface temperature dataset based on direct observations that was used to produce Table 1. NCEP–NCAR reanalysis data were provided through the NOAA Climate Diagnostics Center, and ECHAM4/OPYC3 data were kindly provided by E. Roeckner and M. Esch. This study was supported by the German Research Foundation through the Sonder-forschungsbereich 460 ''Dynamics of Thermohaline Circulation Variability'' and by the Volkswagen Stiftung through the project ''North Atlantic Oscillation: Regional Impacts on European Climate.'' T. Jung benefitted from the computer resources at ECMWF.

REFERENCES

Bjerknes, J., 1964: Atlantic air–sea interaction. *Advances in Geophysics,* Vol. 10, Academic Press, 1–82.

Cayan, D. R., 1992a: Latent and sensible heat flux anomalies over the northern oceans: The connection to monthly atmospheric circulation. *J. Climate,* **5,** 354–369.

——, 1992b: Variability of latent and sensible heat fluxes estimated using bulk formulae. *Atmos.–Ocean,* **30,** 1–42.

Cheng, X., G. Nitsche, and J. M. Wallace, 1995: Robustness of low-frequency circulation patterns derived from EOF and rotated EOF analyses. *J. Climate,* **8,** 1709–1720.

Christoph, M., U. Ulbrich, J. M. Oberhuber, and E. Roeckner, 2000: The role of ocean dynamics for low-frequency fluctuations of the NAO in a coupled ocean–atmosphere GCM. *J. Climate,* **13,** 2536–2549.

Curry, R. G., M. S. McCartney, and T. M. Joyce, 1998: Oceanic transport of subpolar climate signals to mid-depth subtropical waters. *Nature,* **391,** 575–577.

Defant, A., 1924: Die Schwankungen der atmosphärischen Zirkulation über dem Nordatlantischen Ozean im 25-jährigen Zeitraum 1881–1905. *Geogr. Ann.,* **6,** 13–41.

Deser, C., and M. L. Blackmon, 1993: Surface climate variability over the North Atlantic ocean during winter: 1900–1989. *J. Climate,* **6,** 1743–1753.

——, J. E. Walsh, and M. S. Timlin, 2000: Arctic sea ice variability in the context of recent atmospheric circulation trends. *J. Climate,* **13,** 617–633.

Dickson, R. R., and Coauthors, 2000: The Arctic Ocean response to the North Atlantic Oscillation. *J. Climate,* **13,** 2671–2696.

Eden, C., and T. Jung, 2001: North Atlantic interdecadal variability: Oceanic response to the North Atlantic Oscillation (1865–1997). *J. Climate,* **14,** 676–691.

——, and J. Willebrand, 2001: Mechanisms of interannual to decadal variability of the North Atlantic circulation. *J. Climate,* **14,** 2266–2280.

Greatbatch, R. J., 2000: The North Atlantic Oscillation. *Stochastic Environ. Res. Risk Assess.,* **14,** 213–242.

Grigoriev, S., S. K. Gulev, and O. Zolina, 2000: Innovative software facilitates cyclone tracking and analysis. *EOS, Trans. Amer. Geophys. Union,* **81,** 170.

Gulev, S. K., O. Zolina, and S. Grigoriev, 2001: Extratropical cyclone variability in the Northern Hemisphere winter from the NCEP/NCAR reanalysis data. *Climate Dyn.,* **17,** 795–809.

——, T. Jung, and E. Ruprecht, 2002: Climatology and interannual variability in the intensity of synoptic-scale processes in the North Atlantic from the NCEP–NCAR reanalysis data. *J. Climate,* **15,** 809–828.

Hann, J., 1890: Zur Witterungsgeschichte von Nord-Grönland, Westküste. *Meteor. Z.,* **7,** 109–115.

Hilmer, M., and T. Jung, 2000: Evidence for a recent change in the link between the North Atlantic Oscillation and Arctic sea ice export. *Geophys. Res. Lett.,* **27,** 989–992.

Hurrell, J. W., 1995a: Decadal trends in the North Atlantic Oscillation: Regional temperatures and precipitation. *Science,* **269,** 676–679.

——, 1995b: Transistent eddy forcing of the rotational flow during northern winter. *J. Atmos. Sci.,* **52,** 2286–2301.

——, 1996: Influence of variations in extratropical wintertime teleconnections on Northern Hemisphere temperature. *Geophys. Res. Lett.,* **23,** 665–668.

——, and H. van Loon, 1997: Decadal variations in climate associated with the North Atlantic Oscillation. *Climatic Change,* **36,** 301–326.

Jones, P. D., and A. Moberg, 2003: Hemispheric and large-scale surface air temperature variations: An extensive revision and an update to 2001. *J. Climate,* **16,** 206–223.

Jung, T., 2000: The North Atlantic Oscillation: Variability and interactions with the North Atlantic Ocean and Arctic sea ice. Institut für Meereskunde Kiel Res. Rep. 315, 117 pp. [Available from T. Jung, ECMWF, Shinfield Park, Reading RG2 9AX, United Kingdom.]

——, and M. Hilmer, 2001: The link between the North Atlantic Oscillation and Arctic sea ice export through Fram Strait. *J. Climate,* **14,** 3932–3943.

Kalnay, E., and Coauthors, 1996: The NCEP/NCAR 40-Year Reanalysis Project. *Bull. Amer. Meteor. Soc.,* **77,** 437–471.

Kistler, R., and Coauthors, 2001: The NCEP–NCAR 50-year reanalysis: Monthly means CD-ROM and documentation. *Bull. Amer. Meteor. Soc.,* **82,** 247–268.

Kodera, K., H. Koide, and H. Yoshimura, 1999: Northern Hemisphere winter circulation associated with the North Atlantic Oscillation and stratospheric polar-night jet. *Geophys. Res. Lett.,* **26,** 443–446.

Kushnir, Y., 1994: Interdecadal variations in North Atlantic surface temperature and associated atmospheric conditions. *J. Climate,* **7,** 141–157.

Kwok, R., and D. A. Rothrock, 1999: Variability of Fram Strait ice flux and North Atlantic Oscillation. *J. Geophys. Res.,* **104,** 5177–5189.

Loewe, F., 1966: The temperature see-saw between western Greenland and Europe. *Weather,* **21,** 241–246.

Lu, J., and R. J. Greatbatch, 2002: The changing relationship between the NAO and northern hemisphere climate variability. *Geophys. Res. Lett.,* **29,** 1148, doi:10.1029/2001GL014052.

Madden, R. A., and R. H. Jones, 2001: A quantitative estimate of the effect of aliasing in climatological time series. *J. Climate,* **14,** 3987–3993.

Nakamura, H., 1996: Year-to-year and interdecadal variability in the activity of intraseasonal fluctuations in the Northern Hemisphere circulation. *Theor. Appl. Climatol.,* **55,** 19–32.

North, G. R., T. L. Bell, and R. F. Cahalan, 1982: Sampling errors in the estimation of empirical orthogonal functions. *Mon. Wea. Rev.,* **110,** 699–706.

Peterson, K. A., R. J. Greatbatch, J. Lu, H. Lin, and J. Jerome, 2002: Hindcasting the NAO using diabatic forcing of a simple AGCM. *Geophys. Res. Lett.,* **29,** 1336, doi:10.1029/2001GL014502.

——, J. Lu, and R. J. Greatbatch, 2003: Evidence of nonlinear dynamics in the eastward shift of the NAO. *Geophys. Res. Lett.,* **30,** 1030, doi:10.1029/2002GL015585.

Roeckner, E., and Coauthors, 1992: Simulation of the present-day climate with the ECHAM model: Impact of model physics and resolution. MPI Rep. 93, Max-Planck-Institut für Meteorologie, Hamburg, Germany, 56 pp.

——, J. M. Oberhuber, A. Bacher, M. Christoph, and I. Kirchner, 1996: ENSO variability and atmospheric response in a global coupled atmosphere–ocean GCM. *Climate Dyn.,* **12,** 737–754.

Simmons, A. J., J. M. Wallace, and G. Branstator, 1983: Barotropic wave propagation and instability and atmospheric teleconnection patterns. *J. Atmos. Sci.,* **40,** 1363–1392.

Trenberth, K. E., and D. A. Paolino, 1980: The Northern Hemisphere sea-level pressure data set: Trends, errors and discontinuities. *Mon. Wea. Rev.,* **108,** 855–872.

——, and J. W. Hurrell, 1994: Decadal atmosphere–ocean variations in the Pacific. *Climate Dyn.,* **9,** 303–319.

Ulbrich, U., and M. Christoph, 1999: A shift of the NAO and increasing storm track activity over Europe due to anthropogenic greenhouse gas forcing. *Climate Dyn.,* **15,** 551–559.

van Loon, H., and J. C. Rogers, 1978: The seesaw in winter temperatures between Greenland and Northern Europe. Part I: General description. *Mon. Wea. Rev.,* **106,** 296–310.

Walker, G. T., 1924: Correlation in seasonal variation of weather, IX. *Mem. Indian Meteor. Dep.,* **24** (9), 275–332.

Wang, B., 1995: Interdecadal changes in El Niño onset in the last four decades. *J. Climate,* **8,** 267–285.

Wanner, H., S. Bronnimann, C. Casty, D. Gyalistras, J. Luterbacher, C. Schmutz, D. B. Stephenson, and E. Xoplaki, 2001: North Atlantic Oscillation—Concepts and studies. *Surv. Geophys.,* **22,** 321–382.